Journal of Agricultural Science (2014), **152**, 464–482. © Cambridge University Press 2013
doi:10.1017/S002185961300049X

MODELLING ANIMAL SYSTEMS RESEARCH PAPER

The development of a dynamic, mechanistic, thermal balance model for *Bos indicus* and *Bos taurus*

V. A. THOMPSON[1], L. G. BARIONI[2], T. R. RUMSEY[3], J. G. FADEL[1] AND R. D. SAINZ[1]*

[1] *Department of Animal Science, University of California, Davis, CA, USA*
[2] *Computational Mathematics Laboratory, Embrapa Agricultural Informatics, Campinas-SP, Brazil*
[3] *Department of Biological and Agricultural Engineering, University of California, Davis, CA, USA*

(*Received 20 March 2012; revised 25 May 2013; accepted 11 July 2013; first published online 22 August 2013*)

SUMMARY

The dynamic model presented in the current paper estimates heat production and heat flow between growing and mature cattle (*Bos indicus* and *Bos taurus*) and the surrounding environment. Heat production was calculated using the NRC (2000) and heat flows between the animal and the environment were based largely on existing models and physical principles. Heat flows among the body core, the skin, the coat and the environment were calculated. Heat flows from and to the environment included solar radiation, long wave radiation, convection and evaporative heat loss. Physiological responses of cattle (sweating, panting and vasodilation) were modelled through mechanistic equations. The model required weather (radiation, temperature, wind and vapour pressure), animal (body-core weight and genotype-specific parameters) and dietary inputs (dry matter intake rates and diet composition) and estimated heat balance and the physiological responses of the animal to within-day weather variation. The current paper has focused on heat stress, although the model was designed to run under both hot and cold climatic conditions. The model developed in the current paper provides researchers and livestock producers with the ability to predict heat stress and to evaluate mitigating procedures.

INTRODUCTION

In cattle, thermal stress from either heat or cold may result in large losses in production. Physiological responses to heat stress include cutaneous vasodilation, sweating, increased respiration and decreased feed intake. An initial reaction to increased environmental temperature is vasodilation, which increases blood flow to the surface of the skin to bring warm blood in close proximity to the skin surface and thus increase heat loss through convection (Finch 1985). Increases in sweating and respiration rate also increase latent heat loss in the animal (Allen 1962; Thomas & Pearson 1986; Gaughan *et al.* 1999). Ultimately, if physiological processes cannot compensate for the excess body-core heat, a decrease in heat production can be achieved through decreased feed intake (Brown-Brandl *et al.* 2003; Beatty *et al.* 2006). Increasing heat loss through increasing vasodilation and respiration and sweating rates also increases the maintenance requirement for the animal, and decreasing feed intake further limits the amount of energy and nutrients directed towards tissue growth or milk production. The increased maintenance requirement and decreased intake lead to a decrease in animal performance (Blackshaw & Blackshaw 1994; Mitloehner & Laube 2003), which results in an economic loss for producers.

Because of the economic losses associated with heat stress, temperature–humidity indices (THI) were created to estimate level of heat stress of the animal. The THI, proposed by Thom & Bosen (1959), takes into account temperature and humidity to determine the level of heat stress for the animal. However, these indices do not account for physical processes behind the phenomena and therefore have limited capacity in predicting dynamic changes in body-core temperature, physiological and production responses and in evaluating different mitigation options. Therefore, a model that simulates heat flow between the animal and its environment, and heat production by the

* To whom all correspondence should be addressed. Email: rdsainz@ucdavis.edu

animal, can be useful to understand mechanisms of thermal stress, improve prediction of losses in animal performance and, therefore, evaluate the effectiveness of possible management interventions.

The objective of the current work was the creation of a dynamic, mechanistic model to:

- estimate major flows of heat into and out of a bovine
- use heat balance to calculate changes in body-core temperature for growing and mature *B. indicus* and *B. taurus* in response to climatic factors: air temperature, relative and vapour pressure, radiation/shade and wind.

MATERIALS AND METHODS

Model design

A dynamic model, rather than a steady-state model such as that of Turnpenny *et al.* (2000*a*, *b*), was developed since experimental results (e.g. Brown-Brandl *et al.* 2005) have shown that variables such as body-core temperature and respiration rate lag behind changes in environmental variables such as ambient air temperature and incident solar radiation by several hours.

The heat balance model is a three-node model with three state variables: heat contents for body core, skin and coat. Figure 1 shows an overview of the model with all of the flows. A number of three-node heat transfer models have appeared in the literature over the years (see, for example, Porter & Gates 1969; Vera *et al.* 1975; Bakken 1976; McGovern & Bruce 2000). Similar multi-node models have appeared in the human thermal model literature, for example: Stolwijk & Hardy (1966), Gagge *et al.* (1971) and Huizenga *et al.* (2001). The present model is similar to that developed by Gagge *et al.* (1971), which is also known as the Pierce model (Gagge & Gonzalez 2010). The Pierce model is often called a two-node model, although in reality it contains a steady-state energy balance for clothing (for cattle: coat) temperature (Doherty & Arens 1988). The Pierce model continues to be applied in problems such as automobile comfort (Kaynakli & Kilic 2005) and exercise physiology (Takada *et al.* 2009).

All variables, parameters and inputs in the heat balance model are defined in Table 1. The model has three equations (Eqns 1.0, 2.0 and 3.0, in Tables 2 to 4, respectively), with the first two being differential equations and the third being an algebraic equation, and three unknowns: temperature of the body core,

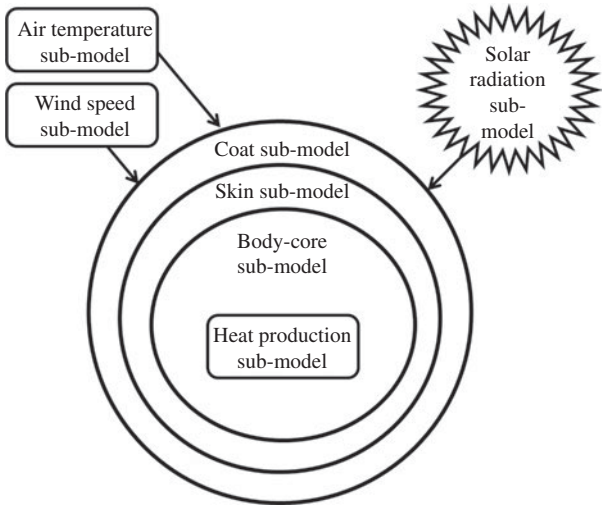

Fig. 1. Overview of the Thompson model. The three concentric circles represent the three layers of the animal: the body-core, skin and coat sub-models. The heat production sub-model is within the body-core. The solar radiation sub-model gives heat to the coat sub-model. The air and wind speed sub-models directly affect all three layers of the animal.

skin and coat (T_b, T_s and T_c, respectively, K). Equation 1.0 represents the change in heat content in the body core (Table 2), Eqn 2.0 represents the change in heat content in the skin layer (Table 3) and Eqn 3.0 represents the heat content balance in the coat (Table 4). Equation 3.0 is similar to that proposed for clothing by Voelker *et al.* (2009) without the evaporation terms. The heat balance model assumes that the storage term in the coat energy balance is small and can be neglected. This is similar to the assumption made for clothing in the early human thermal models (Huizenga *et al.* 2001). Thus, the change in heat content for the coat layer (Eqn 3.0) is set to zero. All of the heat fluxes on the right-hand side of Eqns 1.0, 2.0 and 3.0 are either functions of T_b, T_s and T_c or known functions of time under ambient weather conditions. Heat transfer from appendages (head and legs) is accounted for through skin and coat surface area. The heat transfer through the skin and coat are multiplied by the total surface area, which includes appendages and the dewlap. The assumption is that the resistance within the coat, skin and body core are uniform and thus an average value can be multiplied by the total surface area to represent total heat flows.

Model energy balances were derived using a 'physical formulation' of the finite-difference method for one-dimensional transient conduction problems (Myers 1971). The model assumes that the temperatures in the body core, skin and coat layer are

Table 1. *Description of all variables, parameters and inputs used in the model*

Symbol	Name	Units
A	Surface area of animal	m^2
a	Time lag in maximum wind speed after noon, 1·24 (Hasson *et al.* 1990)	h
A_h	Shadow area cast by animal	m^2
a_{rr}	Slope for respiration rate equation	breaths/K/min
a_{sr}	Parameter for sweating rate equation	g/m^2
B	Variable accounting for Julian day in EoT	rad
b	Coefficient that controls wind speed decrease at night, 3·59 (Hasson *et al.* 1990)	Dimensionless
b_A	Animal surface area parameter	$m^2/kg^{0·57}$
BBD	Time from sunrise	h
b_{rr}	Intercept for respiration rate equation	breaths/min
b_{sr}	Parameter for sweating rate equation	K^{-1}
c	Time lag for minimum wind speed after sunrise, 1 (Hasson *et al.* 1990)	h
clf	Cloud cover (index ranging from 0–1)	Dimensionless
cos	Cosine (function)	–
cp	Wind penetrability of the coat, $9·1 \times 10^{-6}$ (Campbell *et al.* 1980)	m
c_{pb}	Specific heat capacity of the body core, 3·4 (Stolwijk & Hardy 1966)	J/kg/K
c_{pc}	Specific heat capacity of the coat	J/kg/K
c_{pr}	Penetrability of the coat by the wind	m
c_{ps}	Specific heat capacity of the skin, 3·47 (Stolwijk & Hardy 1966)	J/kg/K
c_t	Empirical parameter to calculate temperature, 0·39 (Cesaraccio *et al.* 2001)	Dimensionless
d	Diameter of body-core	m
D	Diffusion coefficient of water vapour at 293·15 K, $2·5 \times 10^{-5}$	m^2/s
DDY	Time length in which wind speed is calculated during the day	h
D_j	Julian day	d
D_l	Day length	h
DMI	Dry matter intake, 0·02 kg Intake/kg M_b.	kg/d
DMI_g	Dry matter intake for gain	kg/d
DMI_m	Dry matter intake for maintenance	kg/d
DWT	Daily wind travel	m/s
e	Natural exponential (function)	–
EBW	Empty body weight	kg
elev	Elevation, 500	m
EoT	Equation of time	min
f_c	Form factor	Dimensionless
Gr	Grashof number	Dimensionless
H	Height of the atmosphere, 8000	m
H_0	Sunset hour for current day	h
H_0'	Sunset hour for previous day	h
H_d	Half-day length	rad
H_dE	Heat of digestion	W
HE	Heat production	W
H_eE	Endogenous heat production (fasting heat production)	W
h_m	Height at standard wind speed measurement, 10	m
H_n	Sunrise hour for current day	h
H_p	Sunrise hour for following day	h
hr	Hour of the day	h
H_rE	Heat energy from retained energy (growth)	W
h_x	Mid animal height	m
H_x	Time of maximum temperature for current day	h
H_x'	Time of maximum temperature for previous day	h
J_o	Solar constant, 1350 (Johnson 1954)	W/m^2
k_a	Thermal conductivity of air, 0·0262	W/m/K
k_{maint}	Maintenance coefficient ($8·91 \times 10^{-7}$; NRC 2000)	$W/kg\ EBW^{0·75}$

Table 1. (*Cont.*)

Symbol	Name	Units
l	Coat length	m
ln	Natural log (function)	–
$longd$	Longitude, 120·5 (Duffie & Beckman 1991)	degrees
l_w	Wind penetration of the coat	m
m	Optical air mass number	Dimensionless
M_b	Body-core mass	kg
M_c	Coat mass	kg
ME	Metabolizable energy	J/kg DM
M_s	Skin mass	kg
NE_g	Net energy for gain	J/kg DM
NE_m	Net energy for maintenance	J/kg DM
N_l	Night length	h
Nu	Nusselt number	Dimensionless
P	Atmospheric air pressure	Pa
p	Coat penetration parameter, 1800 (Turnpenny *et al.* 2000*a*)	m^{-1}
P_o	Atmospheric pressure at sea level, $1{\cdot}01 \times 10^5$	Pa
$p_w(T_a)$	Vapour pressure at air temperature	Pa
$p_{w,sat}(T)$	Saturation vapour pressure at temperature T (function, Eqn 1.7)	Pa
$p_{w,sat}(T_a)$	Saturation vapour pressure at air temperature	Pa
$p_{w,sat}(T_b)$	Saturation vapour pressure at body temperature	Pa
$p_{w,sat}(T_s)$	Saturation vapour pressure at skin temperature	Pa
Q_{10}	Ratio of heat production when temperature elevated by 10 K, 2·0 for ungulates (McArthur 1987)	Dimensionless
$q''_{cond,\ b-s}$	Heat flow through conduction from body-core to skin	W/m^2
$q''_{cond,\ s-c}$	Heat flow through conduction from skin to coat	W/m^2
$q''_{conv,\ c-a}$	Heat flow through convection at coat surface	W/m^2
$q''_{evap,\ s-a}$	Heat flow through cutaneous evaporation	W/m^2
$q''_{lw\ rad,\ c-a}$	Heat flow through long wave radiation	W/m^2
$q''_{resp,\ b-a}$	Heat flow through respiratory loss	W/m^2
$q''_{solar,\ a-c}$	Heat flow through solar energy absorption	W/m^2
r'_R	Resistance of radiation	s/m
r_b	Resistance of conduction; 400 (Turnpenny *et al.* 2000*a*)	s/m
r_{ch}	Resistance through coat	s/m
r_{CH0}	Resistance through coat with no wind	s/m
r_d	Resistance of free convection	s/m
R	Correction factor for variation of earth-sun distance throughout the year	rad
R_{diff}	Diffuse radiation	W/m^2
R_{dir}	Direct radiation	W/m^2
Re	Reynolds number	Dimensionless
R_g	Radiation reaching the ground	W/m^2
R_{gd}	Daily global radiation	$J/m^2/d$
R_{gh}	Hourly radiation reaching the earth's surface	W/m^2
r_H	Resistance to convection	s/m
R_{od}	Daily extraterrestrial radiation	$J/m^2/d$
R_{oh}	Hourly extraterrestrial radiation	W/m^2
RR	Respiration rate	breaths/s
RR_{min}	Respiration rate minimum (12, compiled data)	breaths/min
r_s	Resistance to heat transfer from body-core to skin	s/m
$r_{s,max}$	Maximum resistance to heat transfer from body-core to skin ($36{\cdot}6 \times M_b^{0{\cdot}33}$; Bruce & Clark 1979)	s/m
$r_{s,\min}$	Minimum resistance to heat transfer from body-core to skin (19, Finch 1985)	s/m
r_v	Resistance to cutaneous water vapour transfer	s/m
r_{vl}	Resistance to respiratory water vapour transfer	s/m
sin	Sine (function)	–

Table 1. (*Cont.*)

Symbol	Name	Units
SR	Sweating rate	g/m$^{2/}$h
SSN	Wind speed at sunset	m/s
St	Standard time	h
$stdmer$	Standard meridian for local time zone (120° for Davis, CA)	degrees
T	Temperature	K
t	Time	s
$T(t)$	Air temperature at a given time (t)	K
T_0	Temperature at sunset for current day	K
T_0'	Temperature at sunset for previous day	K
tan	Tangent (function)	–
T_a	Air temperature	K
$T_a(St)$	Air temperature at time St (function)	K
T_b	Body core temperature	K
T_{bref}	Reference body-core temperature, 311·65	K
T_c	Coat temperature	K
T_{dp}	Dew point temperature	K
T_g	Radiant temperature of the ground	K
$timediff$	Difference between solar and standard time	h
T_{mid}	Average of coat and skin temperatures	K
T_n	Minimum temperature for current day	K
T_p	Minimum temperature for following day	K
T_r	Radiant temperature of surroundings	K
T_s	Skin temperature	K
T_{sky}	Radiant temperature of the sky	K
T_{va}	Virtual temperature of the air	K
T_{vb}	Virtual temperature of the body-core	K
T_{vdif}	Difference in virtual temperatures between skin and air	K
T_x	Maximum temperature for current day	K
T_x'	Maximum temperature for previous day	K
u	Wind speed at mid-animal height	m/s
u_m	Wind speed	m/s
V_t	Tidal volume	l/breath
WSN	Minimum wind speed	m/s
WSX	Maximum wind speed	m/s
α	Altitude angle	rad
β	Parameter accounting for body curvature	Dimensionless
γ	Psychrometer constant, 66	Pa/K
δ	Solar declination	rad
ε_c	Coat emissivity, 0·98 (da Silva 2000)	Dimensionless
ε_g	Ground emissivity, 0·98 (da Silva 2000)	Dimensionless
ε_r	Environment emissivity	Dimensionless
ε_{sky}	Sky emissivity	Dimensionless
θ	Solar zenith	rad
λ	Latent heat of vaporization, 2430	J/g
μ	Dynamic viscosity of air	N s/m^2
π	Pi (3·14159)	–
ρ	Density of air	kg/m^3
ρ_c	Coat reflection coefficient (solar radiation)	J reflected/J intercepted
ρc_p	Specific heat of air, 1220	J/m^3/K
ρ_g	Ground reflection coefficient, 0·25 for grass (da Silva 2008)	J reflected/J intercepted
σ	Stefan–Boltzmann constant, $5{\cdot}669\times10^{-8}$	W/m$^{2/}$K^4
τ	Body length of animal, 1·30 (Gaur *et al.* 2002)	m
τ_r	Daily atmospheric transmittance	Dimensionless
ω	Hour angle	rad
ϕ	Latitude, 0·673	rad

Table 2. *Body-core component**

Equation	Description
1.0. $d(M_b \times c_{pb} \times T_b)/\mathrm{d}t = \mathrm{HE} - A(q''_{cond,\ b-s} + q''_{resp,\ b-a})$	Energy balance body-core†, W
1.1. $q''_{cond,\ b-s} = \rho c_p / r_s (T_b - T_s)$	Conduction heat flux from body-core to skin†, W/m^2
1.2. $r_s = \max\{\min\{(T_b - T_{bref}) \times (-30{\cdot}83) + 50, r_{s,\max}\}, r_{s,\min}\}$	Resistance to heat transfer from body-core to skin‡, s/m
1.3. $q''_{resp,b-a} = V_t \times \mathrm{RR} \times \rho c_p (T_{vb} - T_{va})/A + \rho c_p [p_{w,sat}(T_b) - p_w(T_a)]/(\gamma \times r_{vl})$	Heat loss through respiration†§, W/m^2
1.4. $V_t = 2{\cdot}09 \times 10^{-5} \times M_b^{0{\cdot}75} + 5{\cdot}19 \times 10^{-4}$	Tidal volume‖, m^3/breath
1.5. $\mathrm{RR} = \max\{(a_{rr} \times T_b - b_{rr}), \mathrm{RR}_{\min}\}/60$	Respiration rate¶, breaths/s
1.6. $T_{vb} = T_b(1 + 0{\cdot}38 \times p_{w,sat}(T_b)/P)$	Virtual temperature of the body†, K
$T_{va} = T_a(1 + 0{\cdot}38 \times p_{w,sat}(T_a)/P)$	Virtual temperature of the air†, K
1.7. $p_{w,sat}(T) = 6{\cdot}11 \times 10^2 \times \mathrm{e}^{17{\cdot}27(T-273{\cdot}2)/(T-35{\cdot}86)}$	Saturation vapour pressure at temperature T**, Pa
1.8. $P = P_o \times \mathrm{e}^{(-elev/H)}$	Atmospheric pressure††, Pa
1.9. $r_{vl} = \left[2{\cdot}7 \times 10^{-6} \times RR + 5{\cdot}0 \times 10^{-5}\right]^{-1}$	Resistance to water vapour transfer in lungs†, s/m
1.10. $\mathrm{HE} = H_eE + H_dE + H_rE$	Heat production, W
1.11. $H_eE = k_{maint} \times \mathrm{EBW}^{0{\cdot}75} \times Q_{10}^{(T_b - T_{bref})/10}$	Endogenous heat production‡‡, W
1.12. $H_dE = \mathrm{DMI}_m(\mathrm{ME} - \mathrm{NE}_m)/8{\cdot}64 \times 10^4$	Heat energy of digestion, W
1.13. $H_rE = \mathrm{DMI}_g(\mathrm{ME} - \mathrm{NE}_g)/8{\cdot}64 \times 10^4$	Heat energy from retained energy, W
1.14. $\mathrm{DMI}_m = \dfrac{H_eE}{\mathrm{NE}_m}$	Dry matter intake for maintenance, kg DM/s
1.15. $\mathrm{DMI}_g = \mathrm{DMI} - \mathrm{DMI}_m$	Dry matter intake for gain, kg DM/s
1.16. $\mathrm{NE}_g = 1{\cdot}42 \times \mathrm{ME} - 4{\cdot}16 \times 10^{-8} \times \mathrm{ME}^2 + 6{\cdot}96 \times 10^{-16} \times \mathrm{ME}^3 - 6{\cdot}91 \times 10^6$	Net energy for gain, J/kg DM
1.17. $\mathrm{NE}_m = 1{\cdot}37 \times \mathrm{ME} - 3{\cdot}30 \times 10^{-8} \times \mathrm{ME}^2 + 5{\cdot}99 \times 10^{-16} \times \mathrm{ME}^3 - 4{\cdot}69 \times 10^6$	Net energy for maintenance, J/kg DM

* All symbols, variables and parameters are described in Table 1.
† McArthur (1987).
‡ Finch (1985).
§ McGovern & Bruce (2000).
‖ Empirically fit equation.
¶ Thompson *et al.* (2011).
** Murray (1967).
†† Olson (1962).
‡‡ Eqns (1.10) to (1.17): (NRC 2000).

uniform, similar to Crosbie *et al.* (1961) and Stolwijk & Hardy (1966). The equations that represent the change in heat content of the body core, skin and coat layers (Eqns 1.0, 2.0 and 3.0, respectively; all in W), with respect to time are as follows:

$$\mathrm{d}(M_b \times c_{pb} \times T_b)/\mathrm{d}t = \mathrm{HE} - A(q''_{cond,\ b-s} + q''_{resp,\ b-a}) \quad (1.0)$$

$$\mathrm{d}(M_s \times c_{ps} \times T_s)/\mathrm{d}t = A(q''_{cond,\ b-s} - q''_{cond,\ s-c} - q''_{evap,\ s-a}) \quad (2.0)$$

$$\mathrm{d}(M_c \times c_{pc} \times T_c)/\mathrm{d}t = 0 = A(q''_{cond,\ s-c} + q''_{solar,\ a-c} - q''_{conv,\ c-a} - q''_{lw\ rad,\ c-a}) \quad (3.0)$$

More detailed mathematical descriptions of the above equations are presented below and in Tables 2 to 4.

Body-core layer

The energy balance for the body core is described in Table 2. The heat fluxes are modelled using constitutive equations taken from the literature. The body-core heat content is a function of heat production (HE, W; W = J/s; Eqn 1.10, Table 2) and exchanges with the skin and environment by means of conduction and respiration, respectively.

The flow of heat from the body core to the skin, $q''_{cond,\ b-s}$ (W/m^2; Eqn 1.1) was modelled with

Table 3. *Skin layer component**

Equation	Description
2.0. $d(M_s \times c_{ps} \times T_s)/\mathrm{d}t = A\,(q''_{cond,\,b-s} - q''_{cond,\,s-c} - q''_{evap,\,s-a})$	Energy balance skin layer†, W
2.1. $q''_{cond,\,s-c} = \beta \times \rho c_p (T_s - T_c)/r_{ch}$	Heat flux via conduction from coat to skin‡, W/m^2
2.2. $q''_{evap,\,s-a} = \min \begin{cases} \lambda \times a_{sr} \times e^{b_{sr} \times T_s} \\ \rho c_p [p_{w,\,sat}(T_s) - p_w(T_a)]/(\gamma \times r_v) \end{cases}$	Heat flux via evaporation through sweating from skin to ambient§ ‖, W/m^2
2.3. $r_v = (l - l_w)/(D\,(1 + 1{\cdot}54((l - l_w)/d)\,T_{vdif}^{0{\cdot}7}))$	Resistance to water vapor transfer¶, s/m
2.4. $l_w = \dfrac{cp \times u}{\left(cp \times \dfrac{u}{l}\right) + [r_{CH0}]^{-1}}$	Wind penetration of the coat[g], m
2.5. $r_{CH0} = \left[\dfrac{1}{r_d} + \dfrac{1}{r_b} + \dfrac{1}{r'_R}\right]^{-1}$	Resistance through the coat with no wind‡, s/m
2.6. $r_d = \dfrac{\rho c_p}{k_a} \times l$	Resistance of free convection‡, s/m
2.7. $r'_R = \dfrac{3 \times p \times l \times \rho c_p}{16 \times \sigma \times T_{mid}^3}$	Resistance of radiation**, s/m
2.8. $\beta = \dfrac{(1 - l/d)\,\tau + (d - 2 \times l)}{(\tau + d)}$	Body curvature parameter††, dimensionless
2.9. $r_{ch} = \left[\dfrac{1}{r_{CH0}} + c_{pr} \times u\right]^{-1}$	Resistance through coat due to thermal properties††, s/m

* All symbols, variables and parameters are described in Table 1.
† References: (McArthur 1987).
‡ Turnpenny *et al.* (2000*a*).
§ Thompson *et al.* (2011).
‖ Monteith & Unsworth (2008).
¶ Cena & Monteith (1975).
** Cena & Clark (1978).
†† McArthur & Monteith (1980).

a standard heat flow equation (McArthur 1987), which is a function of the temperatures of the body core and skin (T_b and T_s, K) and the resistance to heat transfer (r_s, s/m; Eqn 1.2). The effect of vasodilation/vasoconstriction is represented by r_s; it has a linear relationship with the difference between the reference body-core temperature (T_{bref}; 311·65 K) and the actual body-core temperature and is constrained by minimum and maximum values (Finch 1985).

The heat loss through respiration, $q''_{resp,b-a}$ (W/m^2; Eqn 1.3), is split into convection and evaporation. The heat lost through respiratory convection is a function of tidal volume (V_t; m^3/breath; Eqn 1.4), respiration rate (RR; breaths/s; Eqn 1.5), the specific heat of air (ρc_p; 1220 J/m^3/K), surface area (A; m^2) and the virtual temperatures of the body core and air (T_{vb} and T_{va}; K) (McGovern & Bruce 2000). Virtual body core and air temperatures (Eqn 1.6) depend on saturation vapour pressure ($p_{w,sat}(T)$); Pa; Eqn 1.7), atmospheric air pressure (P; Pa; Eqn 1.8) and temperature (T; K) (McArthur 1987). The $p_{w,sat}(T)$ function is evaluated through the Magnus Tetens equation (Murray 1967) for any temperature variable, i.e. the T argument may assume the values of T_b or T_s.

The calculation for V_t is derived from an equation by McGovern & Bruce (2000), which has a working temperature range from 15 to 40 °C. The genotype-specific parameter values used in the calculation of RR were obtained from a meta-analysis of a wide range of literature data (Thompson *et al.* 2011). Estimates of these parameter values are as follows: *B. taurus,* $a_{rr} = 0{\cdot}6212$ and $b_{rr} = 192{\cdot}7$; *B. indicus,* $a_{rr} = 0{\cdot}7303$ and $b_{rr} = 227{\cdot}2$ (a_{rr}, slope for respiration rate equation, breaths/K/min; b_{rr}, intercept for respiration rate equation, breaths/min).

The heat loss by evaporation from the lungs is modelled following McArthur (1987), using the psychrometer constant (γ; 66 Pa/K), the saturation vapour pressure of the body core ($p_{w,sat}(T_b)$; Pa; Eqn 1.7), the vapour pressure of the air ($p_w(T_a)$;

Table 4. *Coat layer component**

Equation	Description
3.0. $d(M_c \times c_{pc} \times T_c)/\mathrm{d}t = A\,(q''_{cond,\,s-c} + q''_{solar,\,a-c} - q''_{conv,\,c-a} - q''_{lw\,rad,\,c-a})$	Energy balance coat layer†, W
3.1. $q''_{conv,\,c-a} = \rho c_p / r_H (T_c - T_a)$	Heat flux via convection from coat to ambient†, W/m^2
3.2. $r_H = \rho c_p \times d/(k_a \times Nu)$	Resistance to convection†, s/m
3.3. $Nu = max(0{\cdot}48 \times Gr^{0{\cdot}25}, 0{\cdot}24 \times Re^{0{\cdot}6})$	Nusselt number‡, dimensionless
3.4. $Re = \rho \times u \times d/\mu$	Reynolds number‡, dimensionless
3.5. $Gr = \begin{bmatrix} 9{\cdot}81 \times P \times abs(T_s - T_a) + 61\times \\ abs(p_w(T_s) \times T_s - p_w(T_a) \times T_a) \end{bmatrix} / (2{\cdot}73 \times P \times \mu^2)$	Grashof number‡, dimensionless
3.6. $\mu = -3{\cdot}39 \times \mathrm{e}^{-11} \times T^2 + 6{\cdot}77 \times \mathrm{e}^{-8} \times T + 1{\cdot}23 \times \mathrm{e}^{-6}$	Dynamic viscosity of air§, N s/m^2
3.7. $\rho = 1{\cdot}42 \times 10^{-5} \times T^2 - 1{\cdot}28 \times 10^{-2} \times T + 3{\cdot}75$	Density of air§, kg/m^3
3.8. $q''_{solar,\,a-c} = (1 - \rho_c) \times \left[f_c \times R_{dir} + 0{\cdot}5(R_{diff} + \rho_g(R_{dir} + R_{diff})) \right]$	Heat flux via solar radiation from ambient to coat†, W/m^2
3.9. $q''_{lw\,rad,c-a} = \sigma \times \varepsilon_c \times \varepsilon_r (T_c^4 - T_r^4)$	Long wave radiation flux‖, W/m^2
3.10. $\varepsilon_r = (\varepsilon_{sky} + \varepsilon_g)/2$	Emissivity of surroundings‖, dimensionless
3.11. $\varepsilon_{csky} = 1{\cdot}24 \left(\frac{p_w(T_a) \times 10^2}{T_a} \right)^{\frac{1}{7}}$	Clear sky emissivity¶, dimensionless
3.12. $\varepsilon_{sky} = clf + (1 - clf) \times \varepsilon_{csky}$	Sky emissivity**, dimensionless
3.13. $T_r = (T_{sky} + T_g)/2$	Radiant temperature of environment‖, K
3.14. $T_{sky} = T_a \left(\begin{matrix} 0{\cdot}71 + 5{\cdot}6 \times 10^{-3} \times T_{dp} + 7{\cdot}3 \times 10^{-5} \times T_{dp}^2 \\ +0{\cdot}013 \times \cos\left(15 \times St \times \frac{\pi}{180}\right) \end{matrix} \right)^{0{\cdot}25}$	Radiant sky temperature††, K
3.15. $T_g = (1{\cdot}36 \times T_a - 2{\cdot}36) \times (0{\cdot}075 \times ln(R_{gh}) - 0{\cdot}56)$	Radiant ground temperature‡‡, K
3.16. $T_{dp} = \frac{237{\cdot}7\,(ln(p_w(T_a)/0.61))}{17.27 - ln(p_w(T_a)/0.61)} + 273{\cdot}2$	Dew point temperature§§, K
3.17. $f_c = \frac{A_h}{A}$	Form factor‡, dimensionless
3.18. $A = 0{\cdot}14 \times M_b^{0{\cdot}57}$	Surface area‖‖, m^2
3.19. $A_h = \frac{\left(\frac{d}{2}\right)^2 \pi}{\cos(\pi/2 - \alpha)} + (\tau - d)d$	Shadow area of animal¶¶, m^2
Solar radiation sub-model***	
3.20. $R_{dir} = R_{gh} - R_{diff}$	Direct radiation, W/m^2
3.21. $R_{diff} = 0{\cdot}3\,(1 - \tau_r^m) R_{oh}$	Diffuse radiation, W/m^2
3.22. $R_{gh} = \tau_r \times R_{oh}$	Radiation reaching the earth's surface, W/m^2
3.23. $R_{oh} = J_o \times R \times \cos(\theta)$	Extraterrestrial radiation, W/m^2
3.24. $\tau_r = R_{gd}/R_{od}$	Daily atmospheric transmittance, dimensionless
3.25. $R_{od} = 117{\cdot}5 \times 10^6 \times R^2 (H_d \times \sin(\phi) \times \sin(\delta) + \cos(\phi) \times \cos(\delta) \times \sin(H_d))/\pi$	daily extraterrestrial radiation, J/m^2/d
3.26. $\delta = -23{\cdot}5 \times \cos(2 \times \pi\,(D_j + 10)/365)\,\pi/180$	Solar declination, rad
3.27. $H_d = D_l/24 \times \pi$	Half-day length, h
3.28. $D_l = \cos^{-1}(-\tan(\delta) \times \tan(\phi))180/\pi \times 2/15$	Day length, h
3.29. $R = 1 + 0{\cdot}033 \times \cos(2 \times \pi \times D_j/365)$	Sun's radius vector, rad

Table 4. (*Cont.*)

Equation	Description
3.30. $\sin(\alpha) = \sin(\delta) \times \sin(\phi) + \cos(\delta) \times \cos(\phi) \times \cos(\omega)$	Altitude angle, rad
3.31. $\omega = 15\,(St - 12)\,\pi/180$	Hour angle, rad
3.32. $\theta = \pi/2 - \alpha$	Solar zenith, rad
3.33. $m = (P/P_o)/\sin(\alpha)$	Optical air mass number, dimensionless

* All symbols, variables and parameters are described in Table 1.
† Turnpenny *et al.* (2000*a*).
‡ Monteith & Unsworth (2008).
§ Empirically fit equations.
‖ da Silva (2000).
¶ (Brutsaert 1975).
** Crawford & Duchon (1999).
†† Duffie & Beckman (1991).
‡‡ Turco *et al.* (2008).
§§ derived from Magnus Tetens equation; Murray (1967).
‖‖ Brody (1945).
¶¶ Geometric calculation.
*** All solar radiation equations are from Duffie & Beckman (1991) and Oyarzun *et al.* (2007).

Pa; model input), and the resistance to water vapour transfer in the lungs (r_{vl}; s/m; Eqn 1.9). McGovern & Bruce (2000) presented an equation for respiratory evaporative heat loss, but unlike that for convective loss, it greatly overpredicted heat loss. Therefore, McArthur's equation for respiratory evaporation is used in the model.

Heat production (HE; W; Eqn 1.10, Table 2) is modelled with the use of equations adapted from the NRC (1984), where H_eE is endogenous heat production (W), H_dE is heat energy of digestion (W), and H_rE is heat energy from retained energy (W; Eqns 1.10 to 1.13). Heat energy of digestion and from retained energy are calculated from metabolizable energy (ME; J/kg DM), net energies for gain (NE_g, J/kg DM; Eqn 1.16) and maintenance (NE_m, J/kg DM; Eqn 1.17) of the diet (NRC 2000).

Skin layer

The equations for the skin layer sub-model are shown in Table 3. The flow of heat from the skin to the coat ($q''_{cond,\,s-c}$; W/m^2; Eqn 2.1) is a function of body curvature (β; dimensionless; Eqn 2.8), resistance of flow due to coat thermal properties (r_{ch}; s/m; Eqn 2.9) and wind speed (u; m/s; Eqn W1.0 (Table 5); McArthur & Monteith 1980), where c_{pr} is penetrability of the coat by the wind ($2{\cdot}4 \times 10^{-5}$ m) and r_{CH0} is resistance of the coat in still air (s/m; Eqn 2.5).

Cutaneous evaporation

Latent heat loss from the surface of the animal is limited by either its sweating rate or its potential evaporation rate, depending on environmental conditions. Therefore, the minimum values of the functions for sweating and potential evaporation rates are used to model latent heat loss from cutaneous evaporation ($q_{evap,s-a}$; W/m^2; Eqn 2.2), where the upper equation represents the heat loss due to sweating rate and the lower represents the maximum heat loss given the potential evaporation rate, which is subject to environmental conditions.

The maximum evaporation rate is a function of temperature, wind and vapour pressure, where $p_{w,sat}(T_s)$ (Pa; Eqn 1.7) is the saturation vapour pressure of the skin and r_v is the resistance to water vapour transfer (s/m; Eqn 2.3). The equation for r_v is a function of coat length (l; m) and body-core diameter (d; m) (Turnpenny *et al.* 2000*b*).

The sweating rate for the animal is modelled using an empirical equation that has species-dependent parameters obtained from a meta-analysis of a wide range of data from the literature (Thompson *et al.* 2011). This equation was obtained through regressions of sweating data *v.* skin temperature for both *B. taurus*

Table 5. *Wind sub-model used in Tables 3 and 4**

Equation	Description
W1.0. $u = u_m\left(\frac{h_x}{h_m}\right)^{0.14}$	Wind speed at mid-animal height†, m/s
W1.1. $h_x = 0{\cdot}50 + 1{\cdot}21 \times 10^{-3} \times M_b - 1{\cdot}16 \times 10^{-6} \times M_b^2$	Mid animal height‡, m
W1.2. $u_m = \begin{cases} (\mathrm{WSX} - \mathrm{WSN}) \times \sin\left(\frac{\pi \times \mathrm{BBD}}{D_l + 2 \times a}\right) + \mathrm{WSN}, & (H_n + c \leqslant St < H_o) \\ \mathrm{WSN} + (\mathrm{SSN} - \mathrm{WSN}) \times \mathrm{e}^{\left(-b \times \frac{\mathrm{BBD}}{N_l}\right)}, & (St < H_n + c \text{ or } H_o \leqslant St) \end{cases}$	Wind speed§, m/s
W1.3. $\mathrm{WSX} = 1{\cdot}58 + 1{\cdot}18 \times \mathrm{DWT}$	Maximum wind speed§, m/s
W1.4. $\mathrm{WSN} = 0{\cdot}19 + 0{\cdot}58 \times \mathrm{DWT}$	Minimum wind speed§, m/s
W1.5. $\mathrm{SSN} = (\mathrm{WSX} - \mathrm{WSN}) \times \sin\left(\frac{\pi \times \mathrm{DDY}}{D_l + 2 \times a}\right) + \mathrm{WSN}$	Wind speed at sunset§, m/s
W1.6. $\mathrm{DDY} = D_l - c$	Length of day wind speed§, h
W1.7. $\mathrm{BBD} = \begin{cases} 24 - Ho + St, & (St < H_n + c) \\ St - (H_n + c), & (H_n + c \leqslant St < H_o) \\ St - H_o, & (H_o \leqslant St) \end{cases}$	Time from sunrise§, h

* All symbols, variables and parameters are described in Table 1.
† Albright (1990).
‡ ASABE (2006).
§ Peterson & Parton (1983) and Hasson *et al.* (1990).

and *B. indicus*. The parameter values for *B. taurus* and *B. indicus* are $a_{sr} = 2{\cdot}75 \times 10^{-18}$, $b_{sr} = 0{\cdot}147$ and $a_{sr} = 3{\cdot}93 \times 10^{-18}$, $b_{sr} = 0{\cdot}222$, respectively (a_{sr}, g/m^2; b_{sr}, per K).

Skin thickness is used to calculate the skin mass. There are species differences in skin thickness (Pan 1963), but these had no impact on the heat balance for the two species, thus skin thickness was kept at a constant value.

Coat layer

The coat layer sub-model is shown in Table 4. Conduction loss through the ground is not included in this model. The animal is most likely to be standing while heat stressed and in this position there is minimal contact with the ground, making conduction loss negligible. Moreover, O'Connor & Spotila (1992) explain that conduction loss calculations are often difficult, rendering the results inaccurate, and thus are usually omitted from animal heat balance models.

The surface area of the animal, A (m^2; Eqn 3.18), is calculated with the use of the equation developed for *B. taurus* (Brody 1945) and is a function of body-core mass (M_b; kg) and an animal surface area parameter, b_A (0·140 m^2/kg$^{0{\cdot}57}$). Johnston *et al.* (1958) found that *B. indicus* have *c*. 12% more surface area than do *B. taurus*, so for *B. indicus* the parameter $b_A = 0{\cdot}157$ m^2/kg$^{0{\cdot}57}$.

Long-wave radiation

Long-wave radiation ($q''_{lw\ rad}$; W/m^2; Eqns 3.9 to 3.15) is a function of the emissivities and radiant temperatures of the animal and surroundings and the Stefan–Boltzmann constant (σ; W/m^2/K^4). The emissivities in the infrared are given by ε_c, for the surface of the animal (0·98; da Silva 2000), and by ε_r, for the environment, the latter being the average of the ground (ε_g; dimensionless; 0·98 for vegetation; da Silva 2000), and sky emissivities (ε_{sky}; dimensionless). Sky emissivities is calculated as a function of $p_w(T_a)$, T_a (Brutsaert 1975) and cloud cover (*clf*; index ranging from 0 to 1 where 0 represents clear skies and 1 represents complete cloud cover; Crawford & Duchon 1999).

The coat surface temperature and radiant temperature of the surroundings are given by T_c and T_r (K), respectively: T_r (Eqn 3.13) is calculated as the average of the sky (T_{sky}; Eqn 3.14) and ground (T_g; Eqn 3.15) radiant temperatures (K). Dew point temperature

(T_{dp}; K) is calculated with the use of $p_w(T_a)$, according to the Magnus Tetens equation (Murray 1967).

Convection

Convection at the coat surface ($q''_{conv,\ c-a}$; W/m^2; Eqns 3.1 to 3.7) is calculated with the temperature difference between the coat and air divided by the resistance to convective heat transfer (r_H; s/m; Eqn 3.2). The r_H, which uses the Nusselt number (Nu; dimensionless), is dependent on the animal size and decreases as wind speed increases (Turnpenny *et al.* 2000*a*); Nu (Eqn 3.3) is a function of both wind speed and animal geometry and is calculated with the use of Reynolds (Re, dimensionless; Eqn 3.4) and Grashof (Gr, dimensionless; Eqn 3.5) numbers (Monteith 1973; Incropera & DeWitt 1990; McGovern & Bruce 2000) For natural convection, where $Gr > 16 \times Re^2$, $Nu = 0{\cdot}48 \times Gr^{0{\cdot}25}$. For forced convection, where $Gr < 0{\cdot}1 \times Re^{0{\cdot}6}$, $Nu = 0{\cdot}24 \times Re^{0{\cdot}6}$. Otherwise, when wind speed is low, Nu will be the greater of the two above estimates.

The Re and Gr numbers are functions of wind speed u (m/s; Eqn W1.0, Table 5), animal diameter d (m), the dynamic viscosity of air μ (N s/m^2; Eqn 3.6), and the density of air ρ (kg/m^3; Eqn 3.7). The viscosity and density of air were fitted to equations, both of which are a function of the mean of the skin and air temperatures (K).

The model operates with the assumption that values of daily measurements of minimum and maximum air temperature, maximum solar radiation, vapour pressure (at any time throughout the day) and daily wind travel (DWT) are known.

Solar radiation

Solar radiation absorbed by the animal ($q''_{solar,\ a-c}$; W/m^2; Eqn 3.8) comes from three sources: direct radiation (R_{dir}; Eqn 3.20), diffuse radiation (R_{diff}; Eqn 3.21) and radiation reflected from the ground surface, which is a function of R_{dir} and R_{diff}, all in W/m^2. Absorbed radiation is a function of reflection coefficients for the animal and the ground, ρ_c and ρ_g (J reflected/J intercepted), respectively, and form factor (f_c; dimensionless; Eqn 3.17). Form factor is a function of the animal's body angle in relation to the sun and its body dimensions (Monteith & Unsworth 2008) and is calculated as the quotient of the shadow area of the animal (A_h; m^2; Eqn 3.19) and A. The shadow area of the animal is a function of the animal's body length (τ; m), d and the altitude angle of the sun (α; rad; Eqn 3.30).

The solar radiation sub-model is shown in Table 3 (Eqns 3.20 to 3.33). The calculation of R_{dir} and R_{diff} first requires the calculation of daily extraterrestrial radiation, R_{od} (MJ/m^2/d), with the use of solar declination (δ; rad; Eqn 3.26), latitude (ϕ; rad), half-day length (H_d; rad; Eqn 3.27) and the correction factor for the variation of the earth–sun distance throughout the year (R; rad; Eqn 3.29) (Duffie & Beckman 1991; Oyarzun *et al.* 2007).

Solar declination is the angle of the earth in relation to the sun (0° is reached twice a year at the equinox), based on the Julian day, D_j (1 Jan is 1 and 31 Dec is 365; d; Eqn 3.28). Altitude angle of the sun is the altitude of the sun at any given point throughout the day: at noon on the equator during the equinox it is 90° or $\pi/2$. Solar zenith (θ; rad) is the complement to α. Hour angle (ω; rad; Eqn 3.31) is the daily rotation of the earth at any given hour (where midnight is 0), and is a function of standard time (St; h), which is the hour of the day using a 24-h clock.

The extra-terrestrial radiation, R_{oh} (W/m^2; Eqn 3.23) is calculated with the use of the solar constant, J_o (1350 W/m^2; Johnson 1954). The radiation reaching the earth's surface, R_{gh} (W/m^2; Eqn 3.22) is then calculated with the use of the daily atmospheric transmittance (τ_r; dimensionless; Eqn 3.24) and R_{oh}. τ_r is the ratio of the daily global radiation (R_{gd}; J/m^2/d), which is obtained from data collected through weather stations, to R_{od}. Cloud cover is accounted for through τ_r, which decreases as cloud cover increases. Diffuse radiation increases in proportion to total radiation as cloud cover increases and τ_r decreases.

Diffuse radiation (Eqn 3.21) is a function of τ_r, R_{oh}, and optical air mass number, m (dimensionless; Eqn 3.33). Atmospheric pressure and atmospheric pressure at sea level are given by P (Pa; Eqn 1.8) and P_o ($1{\cdot}01 \times 10^5$ Pa), respectively. Ground elevation is elev (500 m), and H is the height of the atmosphere (8000 m). Direct radiation (Eqn 3.20) is calculated as the difference between R_{gh} and R_{diff}.

Air temperature

The equations used to calculate air temperature (Table 6) come from Cesaraccio *et al.* (2001) and from the variables calculated in the Solar Radiation section (Table 4). Figure 2 shows a sketch of the inputs needed for the air temperature sub-model, where all temperatures are in K and all of the times, St, are

Table 6. *Air temperature sub-model used in Tables 2 to 4* †*

Equation	Description
A1.0. $T_a(St) = \begin{cases} T_0' + \frac{T_n - T_0'}{\sqrt{H_n - H_0'}}\sqrt{St - H_0'}, & (0 < St \leqslant H_n) \\ T_n + (T_x - T_n) \times \sin\left[\frac{\pi}{2}\left(\frac{St - H_n}{H_x - H_n}\right)\right], & (H_n < St \leqslant H_x) \\ T_n + (T_x - T_0) \times \sin\left[\frac{\pi}{2} + \frac{\pi}{2}\left(\frac{St - H_x}{4}\right)\right], & (H_x < St \leqslant H_0) \\ T_0 + \frac{T_p - T_0}{\sqrt{H_p - H_0}}\sqrt{St - H_0} & (H_0 < St \leqslant 24) \end{cases}$	Air temperature at time St, K
A1.1. $H_x = H_0 - 4$	The time of maximum temperature, h
A1.2. $H_n = 12 - D_l/2 - timediff$	Hour of sunrise, h
A1.3. $H_0 = 12 + D_l/2 - timediff$	Hour of sunset, h
A1.4. $timediff = (4\,(stdmer - longd) + \mathrm{EoT})/60$	Difference between solar time and standard time, h
A1.5. $\mathrm{EoT} = 229{\cdot}2\,(7{\cdot}5 \times 10^{-5} + 1{\cdot}87 \times 10^{-3} \times \cos(B) - 0{\cdot}032 \times \sin(B) - 0{\cdot}015 \times \cos(2 \times B) - 0{\cdot}041 \times \sin(2 \times B))$	Equation of time, min
A1.6. $B = \pi\,(D_j - 1)\,2/365$	Variable accounting for Julian day, rad
A1.7. $T_0 = T_x - c_t(T_x - T_p)$	Temperature at sunset for current day, K
A1.8. $T_0' = T_x' - c_t(T_x' - T_p')$	Temperature at sunset for previous day, K

* All symbols, variables and parameters are described in Table 1.
† Eqns (A1.2)–(A1.6) are from Duffie & Beckman (1991), whereas the rest are from Cesaraccio *et al.* (2001).

in hours (h). The air temperature calculation, $T_a(St)$ (Eqn A1.0), is separated into four different parts of the day: from midnight to sunrise (H_n), from H_n to time of maximum air temperature (H_x), from H_x to sunset (H_0) and then from H_0 to midnight.

The difference between solar time and standard time is timediff (h; Eqn A1.4). timediff is calculated with the use of equation of time (EoT; min; Eqn A1.5), standard meridian for local time zone (*stdmer*; 120° for Davis, CA) and longitude (*longd*; 120·5° for Davis, CA) (Duffie & Beckman 1991).

Wind speed

The wind speed sub-model, shown in Table 5, comes from Peterson & Parton (1983), with some revisions by Hasson *et al.* (1990). The inputs for wind speed calculations are DWT (m/s) and Julian day (D_j). Maximum (WSX; m/s; Eqn W1.3) and minimum (WSN; m/s; Eqn W1.4) wind speeds are calculated from DWT (Hasson *et al.* 1990).

Wind speed at mid-animal height (u; m/s; Eqn W1.0) is a function of wind speed (u_m; m/s) at height h_m (m) and mid-animal height (h_x; m). Wind speed is a two-part equation, which has day and night components (Eqn W1.2): u_m during the day (Eqn W1.2) is a function of WSX and WSN, the time from sunrise (BBD; h; Eqn W1.7) and two parameters a and c, which are the lag in maximum wind speed after noon ($a = 1{\cdot}24$; h) and the lag in minimum wind speed after sunrise ($c = 1$; h), respectively. Wind speed at night is a function of WSN, the length of time that the wind speed is calculated during the day (DDY; h; Eqn W1.6), the coefficient that controls wind speed decrease at night ($b = 3{\cdot}59$; dimensionless), day length (D_l; h), night length ($N_l = 24 - D_l$; h) and the wind speed at sunset (*SSN*; m/s; Eqn W1.5) (Hasson *et al.* 1990).

Wind speed at height h_m, is converted into u at h_x with the use of the equation by Albright (1990). Mid-animal height is calculated with the use of a regression equation, which was fit to *B. taurus* data and is multiplied by 1·2 for *B. indicus* (Eqn W1.1; ASABE 2006).

Both air temperature and wind speed sub-models had slope discontinuities, but this did not result in numerical difficulties in the solutions of the model and they compared well with hourly data.

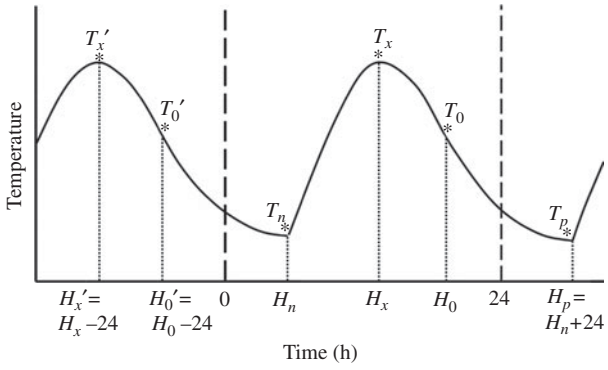

Fig. 2. Sketch of the temperature model (Cesaraccio *et al.* 2001). T_n is the minimum temperature for current day, T_x is the maximum temperature for current day, T_x' is the maximum temperature for previous day, T_0 is the temperature at sunset for current day, T_0' is the temperature at sunset for previous day and T_p is the minimum temperature for following day (all in K). H_n is the sunrise hour for current day, H_0 is the sunset hour for current day, H_0' is the sunset hour for previous day, H_x is the time of maximum temperature for current day, H_x' is the time of maximum temperature for previous day and H_p is the sunrise hour for next day (all in standard time, h).

Model simulation

The model was coded in Matlab (2010) and used a built-in ordinary differential equation solver (ode23t). It is capable of handling systems of differential algebraic equations (DAEs) (Shampine *et al.* 1999), such as Eqns 1.0, 2.0 and 3.0. The climate input data (temperature, vapour pressure, solar radiation and wind speed) were obtained from regional weather stations for 21–24 June 2006 in Davis, CA (CIMIS 2009) as daily inputs (Thompson *et al.* in press). Hourly weather data, if available, can be implemented in the model, replacing the climate equations with interpolation routines.

Animal inputs (shown in Table 7) are species-specific. *Bos indicus* have some adaptations which make them more tolerant to a tropical climate than *B. taurus*, such as a large dewlap, higher sweating rates, lighter coat, change in distribution of body reserves (large hump) and thicker skin (Pan 1963; Hansen 2004). The model accounts for the dewlap with increased surface area. Preliminary analysis showed that the thicker skin of *B. indicus* had no impact on heat balance. The differences in basal metabolic rate have little impact on heat balance (this was fully evaluated with the sensitivity analysis as described in Thompson *et al.* in press). The higher sweating rate and shorter coat are also both accounted for in the animal inputs section. McDowell *et al.* (1958) found that the hump had no impact on heat regulation, thus this was not included in the model. The animal inputs also allow for a wide range of animal maturity from growing to mature cattle. This excludes pre-weaned calves as well as lactating and gestating animals, as such animals would require additional model changes, which may include sweating rates, heat of lactation and metabolic heat production.

RESULTS AND DISCUSSION

As shown in Fig. 3, the patterns for air temperature and wind speed were similar, a pattern also found by Cesaraccio *et al.* (2001), Peterson & Parton (1983) and Hasson *et al.* (1990). The nadir in the diurnal fluctuations occurred at sunrise (or shortly thereafter in the case of wind speed) and the zenith some time after noon and before sunset. The inputs for this figure consisted of climate data from 21 to 24 June 2006 in Davis, CA (CIMIS 2009).

Figure 4 shows the ground level diffuse, direct and total radiation (W/m^2). The peak for diffuse radiation was much flatter than those for direct and total radiation. In the early morning and late afternoon, the sun must travel through more of the earth's atmosphere, and the proportion of diffuse to direct radiation increases as more radiation is 'scattered' (Duffie & Beckman 1991). During the midday hours, although total radiation peaks, a lower proportion of the radiation is diffuse. On the fourth simulation day, the amount of total radiation and direct radiation fell, but the amount of diffuse radiation rose, due to the presence of cloud cover on that day. Cloud cover can increase the proportion of diffuse radiation from 0·1–0·3 to 1·0 of total radiation (Sen 2008).

The simulated evaporation potential (Eqn 2.2) behaved as expected, sharply decreasing at both high temperature and high humidity, as commonly seen in the humid tropics (Fig. 5). Evaporation potential increases as air temperature increases at low relative humidity, because absolute humidity potential increases with air temperature. However, at high relative humidity, the evaporation potential decreases as air temperature increases. At high relative humidity, the vapour pressure gradient decreases as air temperature nears body-core temperature, making it more difficult for the animal to lose water vapour to its surrounding environment.

The long-wave radiation and convection losses (Eqns 3.9 and 3.1, respectively) from the animal are

Table 7. *Animal inputs for Nellore and Angus*

Parameter	Nellore	Angus	References
d – body-core diameter (m)	$0{\cdot}06 \times M_b^{0{\cdot}39}$	$0{\cdot}06 \times M_b^{0{\cdot}39}$	(Ehrlemark 1988; Singh *et al.* 2002)
M_b– body-core mass (kg)	400	400	–
l – coat length (m)	0·002	0·004	(Hutchinson & Brown 1969)
ρ_c – reflection coefficient of coat (dimensionless)	0·51	0·12	(Monteith 1973; da Silva 2008)
a_{rr} – respiration rate parameter (breaths/K/min)	0·62	0·73	(Thompson *et al.* 2011)
b_A – surface area parameter ($m^2/kg^{0{\cdot}57}$)	0·14	0·16	(Brody 1945; Johnston *et al.* 1958)
b_{rr} – respiration rate parameter (breaths/min)	192·7	227·2	(Thompson *et al.* 2011)
a_{sr} – sweating rate parameter (g/m^2)	$2{\cdot}75 \times 10^{-18}$	$3{\cdot}93 \times 10^{-18}$	(Thompson *et al.* 2011)
b_{sr} – sweating rate parameter (per K)	0·15	0·22	(Thompson *et al.* 2011)

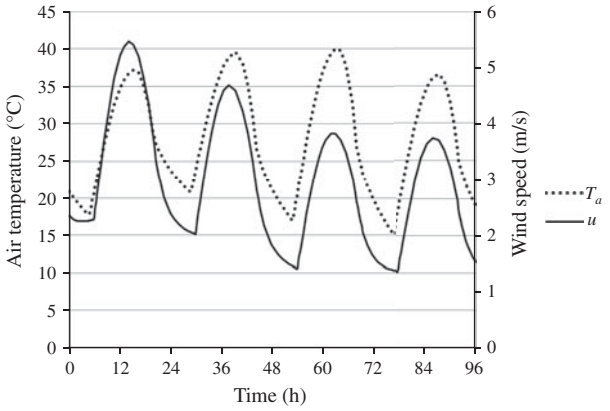

Fig. 3. Air temperature (T_a; °C) and wind speed (u; m/s) over four days. Both lines follow similar diurnal fluctuations with nadirs at sunrise and zeniths in the early afternoon.

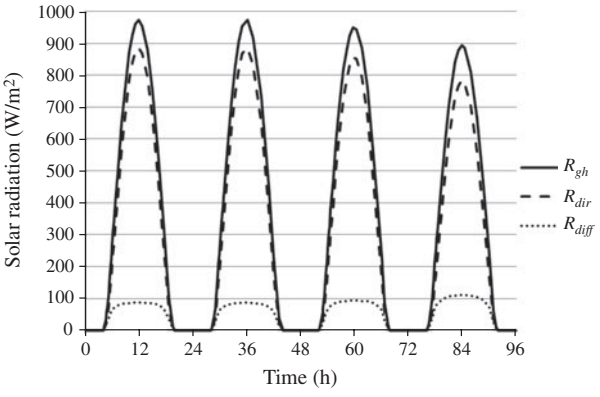

Fig. 4. Solar radiation on a horizontal surface at the ground. Radiation is separated into three lines, total, direct and diffuse (R_{gh}, R_{dir} and R_{diff}, respectively).

shown in Fig. 6 with increasing air temperature (wind speed is zero). The gradient between air and body-core temperatures drives these equations, which are independent of humidity. The difference between the temperature of the animal and its environment increases as air temperature decreases, which increases both the long-wave radiation and the convection losses from the animal. Above 36 °C, both long-wave radiation and convection became negative, indicating a net sensible heat gain by the animal, as also reported by Gebremedhin (1987). Even though Zhang *et al.* (2007) found that humidity increases convection losses, it does so only for objects with temperatures ranging from 77 to 177 °C, which is above the range for the surface of cattle. The increasing humidity resulted in water collecting on surfaces, which then evaporated, resulting in turn in greater sensible heat losses.

Figure 7 shows the surface plot of convective heat loss *v.* air temperature and wind speed. At low air temperature, increasing wind speed increases the convection loss experienced by the animal. Conversely, at high air temperature, increasing wind speed increases convection gain experienced by the animal. The results obtained by McArthur (1991) and Gebremedhin (1987) exhibited similar relationships among convective heat loss, air temperature and wind speed. Wind decreases resistance to convective heat transfer; thus, when the air temperature is low and the animal is losing heat due to convection, increasing wind speed will increase the rate of this loss, and when air temperature is high and the animal is gaining heat due to convection, increasing wind speed will increase the rate of this gain.

The model simulation outputs for *B. taurus* and *B. indicus* are shown in Fig. 8. The points for skin temperature lie between those for body-core and air temperatures, a relationship consistent with findings by Gebremedhin *et al.* (2008), Allen (1962) and Thomas & Pearson (1986). Maia *et al.* (2008) found coat temperatures to be between 2 and 14 °C above air temperature, which is consistent with the results

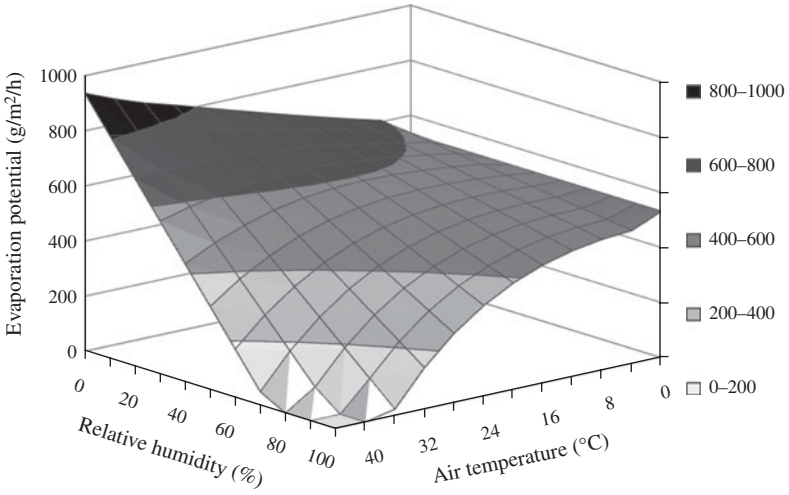

Fig. 5. Simulated evaporation potential of sweat on the skin of cattle *v.* air temperature and relative humidity.

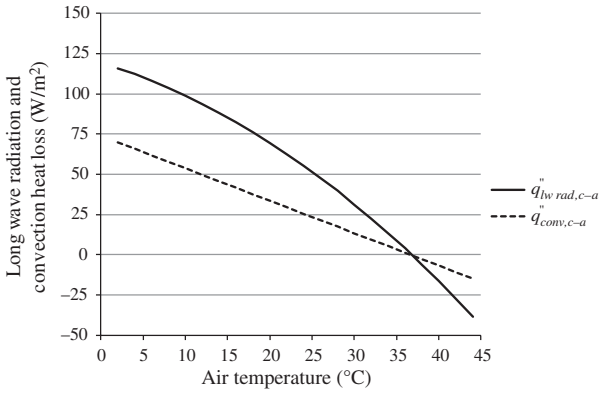

Fig. 6. Long-wave radiation ($q''_{lw\ rad,\,c-a}$) and convection ($q''_{conv,\,c-a}$) losses from cattle at zero wind speed over air temperature (°C).

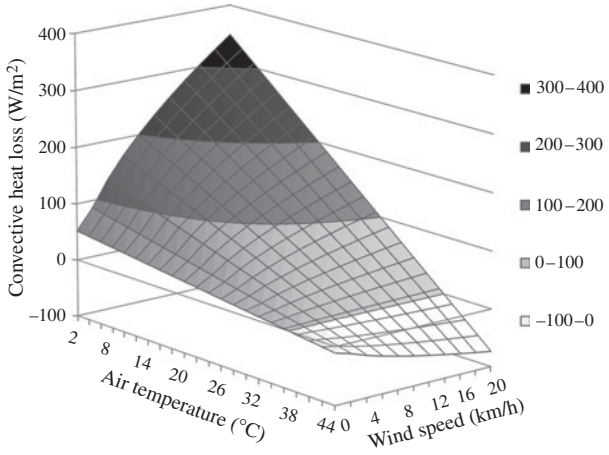

Fig. 7. Convective heat loss from the animal *v.* air temperature and wind speed.

reported for *B. taurus* in the current work. The *B. indicus* body-core, skin and coat temperatures are all lower than the *B. taurus* due to their adaptations to hot climate conditions. For both species, the fluctuations in daily skin and coat temperatures are slightly offset from those in air temperature, due to the impact of solar radiation. Peak air temperature occurred around 15·00 h, while peak solar radiation occurred at midday. The increase in solar load on the animal resulted in an increase in coat temperature slightly before the increase in air temperature, and as soon as air temperature decreased, the solar load was no longer substantial, so the coat temperature could decrease along with air temperature.

Figure 9 shows the heat flows between the animal and its environment for *B. taurus* and *B. indicus*. For *B. taurus*, the highest incoming flow was solar radiation absorption, which exhibited a peak during solar hours around noon. The inputs for this figure consisted of climate data from 21 to 22 June 2006, which includes the summer solstice, around which time incoming solar radiation is the highest for the year (reaching 973 W/m^2 at 12·00 h). *Bos indicus* have lower solar radiation absorption due to higher coat reflectivity. For both species, cutaneous evaporation and respiratory losses account for the majority of heat loss during the day, especially near 16·00 h when air temperature reaches its maximum. Long-wave radiation and convection losses are greatest at night and in the early morning hours, as shown in studies by Kibler & Yeck (1959), Kelly *et al.* (1954) and Gebremedhin (1987), who found that, as air temperature decreases both convection and long wave radiation losses

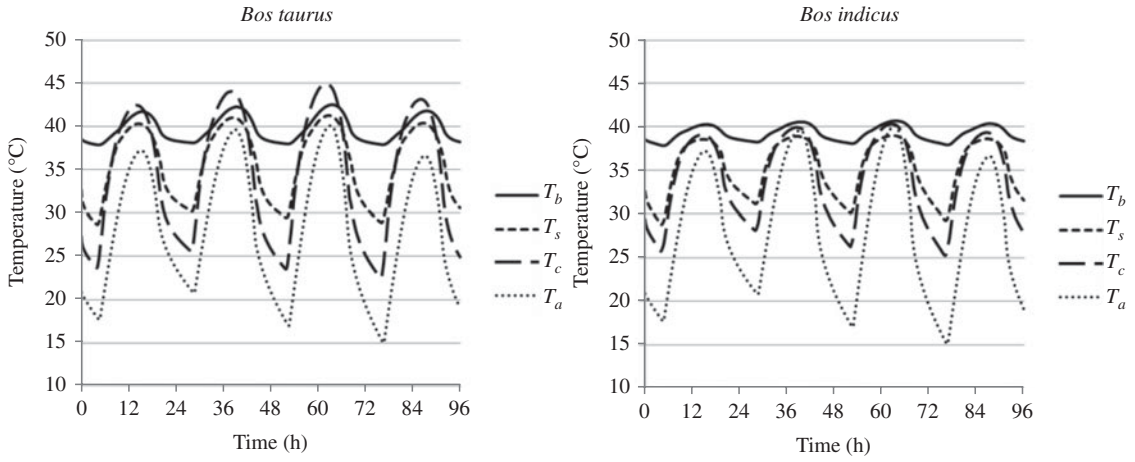

Fig. 8. Simulation outputs for *Bos taurus* and *Bos indicus*. The model was simulated over four days (96 h). The outputs are body-core, T_b, skin, T_s, coat, T_c and air, T_a, temperatures.

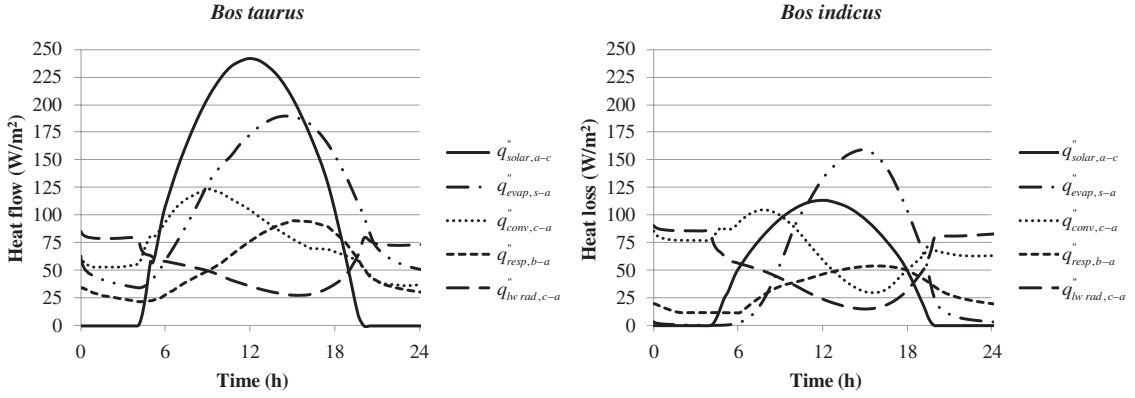

Fig. 9. Heat flows between a *Bos taurus* and *Bos indicus* animal and its environment (W/m^2). The flows are heat loss due to cutaneous evaporation, $q''_{evap,\ s-a}$, solar absorption, $q''_{solar,\ a-c}$, convection losses, $q''_{conv,\ c-a}$, long wave radiation losses, $q''_{lw\ rad,\ c-a}$ and respiration losses, $q''_{resp,\ b-a}$.

increase, whereas evaporative loss decreases. *Bos taurus* and *B. indicus* exhibit similar trends, although the flows for *B. taurus* are generally higher due to higher heat stress and thus increased need to dissipate excess heat.

CONCLUSION

Future development for the current model could be the addition of a dynamic heat production component, which includes eating behaviour, a detailed representation of cloud cover and rainfall, a sprinkler/mister component, which includes droplet size and a heat production component of gestation and lactation.

Although many parts of this model can be evaluated independently, the prediction potential and extensive model analysis will be presented in the subsequent paper (Thompson *et al*. in press). The current model integrates concepts and data relating to heat flows between animals and their environment. The equation forms and parameters are largely based on generally accepted physical, anatomical and physiological principles. Even though this model must be further evaluated against more complete, extensive datasets to assess its ability to predict body-core temperature in response to different environmental conditions for both *B. taurus* and *B. indicus*, the results produced by the model are physiologically sound and follow the trend of known biology.

This research was supported by the Lyons Fellowship, the Jastro Shields Award (V.A.T.) and the W. K. Kellogg Endowment, USDA NIFA Multistate Research Project NC-1040. We gratefully acknowledge

the infrastructure support of the Department of Animal Science, College of Agricultural and Environmental Sciences, the California Agricultural Experiment Station of the University of California, Davis and Embrapa Cerrados, Planaltina, Brazil.

REFERENCES

Albright, L. D. (1990). *Environment Control for Animals and Plants*. St. Joseph, MI, USA: American Society of Agricultural Engineers.

Allen, T. E. (1962). Responses of Zebu, Jersey, and Zebu X Jersey crossbred heifers to rising temperature, with particular reference to sweating. *Australian Journal of Agricultural Research* **13**, 165–179.

American Society of Agricultural and Biological Engineers (ASABE) (2006). *Dimensions of Livestock and Poultry*. ASAE Livestock Dimension and Configuration Factors Subcommittee, ASAE Structures and Environment Division Technical Committee. ASAE Standard D321.2 MAR1985 (R2006). St. Joseph, MI, USA: ASABE.

Bakken, G. S. (1976). A heat transfer analysis of animals: unifying concepts and the application of metabolism chamber data to field ecology. *Journal of Theoretical Biology* **60**, 337–384.

Beatty, D. T., Barnes, A., Taylor, E., Pethick, D., Mccarthy, M. & Maloney, S. K. (2006). Physiological responses of *Bos taurus* and *Bos indicus* cattle to prolonged, continuous heat and humidity. *Journal of Animal Science* **84**, 972–985.

Blackshaw, J. K. & Blackshaw, A. W. (1994). Heat stress in cattle and the effect of shade on production and behaviour: a review. *Australian Journal of Experimental Agriculture* **34**, 285–295.

Brody, S. (1945). *Bioenergetics and Growth: with Special Reference to the Efficiency Complex in Domestic Animals*. New York: Reinhold.

Brown-Brandl, T. M., Nienaber, J. A., Eigenberg, R. A., Hahn, G. L. & Freetly, H. (2003). Thermoregulatory responses of feeder cattle. *Journal of Thermal Biology* **28**, 149–157.

Brown-Brandl, T. M., Eigenberg, R. A., Nienaber, J. A. & Hahn, G. L. (2005). Dynamic response indicators of heat stress in shaded and non-shaded feedlot cattle, Part 1: analyses of indicators. *Biosystems Engineering* **90**, 451–462.

Bruce, J. M. & Clark, J. J. (1979). Models of heat production and critical temperature for growing pigs. *Animal Production* **28**, 353–369.

Brutsaert, W. (1975). Derivable formula for long-wave radiation from clear skies. *Water Resources Research* **11**, 742–744.

Campbell, G. S., McArthur, A. J. & Monteith, J. L. (1980). Windspeed dependence of heat and mass transfer through coats and clothing. *Boundary-Layer Meteorology* **18**, 485–493.

Cena, K. & Clark, J. A. (1978). Thermal insulation of animal coats and human clothing. *Physics in Medicine & Biology* **23**, 565–591.

Cena, K. & Monteith, J. L. (1975). Transfer processes in animal coats. III. Water vapour diffusion. *Proceedings of the Royal Society of London. Series B, Biological Sciences* **188**, 413–423.

Cesaraccio, C., Spano, D., Duce, P. & Snyder, R. L. (2001). An improved model for determining degree-day values from daily temperature data. *International Journal of Biometeorology* **45**, 161–169.

CIMIS (2009). *California Irrigation Management Information System Department of Water Resources*. Sacramento, CA, USA: Office of Water Use Efficiency. Available from: http://wwwcimis.water.ca.gov/cimis/welcome.jsp (verified 30 May 2013).

Crawford, T. M. & Duchon, C. E. (1999). An improved parameterization for estimating effective atmospheric emissivity for use in calculating daytime downwelling longwave radiation. *Journal of Applied Meteorology* **38**, 474–480.

Crosbie, R. J., Hardy, J. D. & Fessenden, E. (1961). Electrical analog simulation of temperature regulation in man. *IRE Transactions on Bio-Medical Electronics* **8**, 245–252.

Da Silva, R. G. (2000). *Introdução à Bioclimatologia Animal*. São Paulo, Brazil: Nobel.

Da Silva, R. G. (2008). *Biofisica Ambiental: Os Animais e seu Ambiente*. São Paulo, Brazil: Funep.

Doherty, T. J. & Arens, E. A. (1988). Evaluation of the physiological bases of thermal comfort models. *ASHRAE Transactions* **94**, 1371–1385.

Duffie, J. A. & Beckman, W. A. (1991). *Solar Engineering of Thermal Processes*. New York: Wiley.

Ehrlemark, A. (1988). *Calculation of sensible heat and moisture loss from housed cattle using heat balance model*. Uppsala, Sweden: Department of Farm Buildings, Swedish University of Agricultural Sciences.

Finch, V. A. (1985). Comparison of non-evaporative heat transfer in different cattle breeds. *Australian Journal of Agricultural Research* **36**, 497–508.

Gagge, A. P. & Gonzalez, R. R. (2010). Mechanisms of heat exchange: biophysics and physiology. In *Comprehensive Physiology* (Ed. R. Terjung), pp. 45–84. New York: John Wiley & Sons, Inc.

Gagge, A. P., Stolwijk, J. A. J. & Nishi, Y. (1971). An effective temperature scale based on a simple model of human physiological regulatory response. *ASHRAE Transactions* **77**, 247–262.

Gaughan, J. B., Mader, T. L., Holt, S. M., Josey, M. J. & Rowan, K. J. (1999). Heat tolerance of Boran and Tuli crossbred steers. *Journal of Animal Science* **77**, 2398–2405.

Gaur, G. K., Kaushik, S. N. & Garg, R. C. (2002). Ongole cattle status in India. *Animal Genetic Resources Information* **32**, 27–34.

Gebremedhin, K. G. (1987). Effect of animal orientation with respect to wind direction on convective heat-loss. *Agricultural and Forest Meteorology* **40**, 199–206.

Gebremedhin, K. G., Hillman, P. E., Lee, C. N., Collier, R. J., Willard, S. T., Arthington, J. & Brown-Brandl, T. M. (2008). Sweating rates of dairy cows and beef heifers in hot conditions. *Transactions of the ASABE* **51**, 2167–2178.

Hansen, P. J. (2004). Physiological and cellular adaptations of zebu cattle to thermal stress. *Animal Reproduction Science* **82–83**, 349–360.

Hasson, A. M., Al-Hamadani, N. I. & Al-Karaghouli, A. A. (1990). Comparison between measured and calculated diurnal variations of wind speeds in northeast Baghdad. *Solar & Wind Technology* **7**, 481–487.

Hutchinson, J. C. D. & Brown, G. D. (1969). Penetrance of cattle coats by radiation. *Journal of Applied Physiology* **26**, 454–464.

Huizenga, C., Hui, Z. & Arens, E. (2001). A model of human physiology and comfort for assessing complex thermal environments. *Building and Environment* **36**, 691–699.

Incropera, F. P. & Dewitt, D. P. (1990). *Fundamentals of Heat and Mass Transfer*. New York: John Wiley and Sons.

Johnson, F. S. (1954). The solar constant. *Journal of Meteorology* **11**, 431–439.

Johnston, J. E., Hamblin, F. B. & Schrader, G. T. (1958). Factors concerned in the comparative heat tolerance of Jersey, Holstein and Red Sindhi-Holstein (F1) cattle. *Journal of Animal Science* **17**, 473–479.

Kaynakli, O. & Kilic, M. (2005). An investigation of thermal comfort inside an automobile during the heating period. *Applied Ergonomics* **36**, 301–312.

Kelly, C. F., Bond, T. E. & Heitman, H. Jr (1954). The role of thermal radiation in animal ecology. *Ecology* **35**, 562–569.

Kibler, H. H. & Yeck, R. G. (1959). *Environmental Physiology and Shelter Engineering with Special Reference to Domestic Animals L: Vaporization Rates and Heat Tolerance in Growing Shorthorn, Brahman and Santa Gertrudis Calves Raised at Constant 50° and 80 °F Temperatures*. Missouri Research Bulletin 701. Columbia, MO, USA: University of Missouri, College of Agriculture Agricultural Experiment Station.

Maia, A. S. C., Da Silva, R. G. & Loureiro, C. M. B. (2008). Latent heat loss of Holstein cows in a tropical environment: a prediction model. *Brazilian Journal of Animal Science* **37**, 1837–1843.

MATLAB (2010). *Matlab Version 7.8.0*. Natick, MA, USA: MathWorks Inc.

McArthur, A. J. (1987). Thermal interaction between animal and microclimate: a comprehensive model. *Journal of Theoretical Biology* **126**, 203–238.

McArthur, A. J. (1991). Thermal-radiation exchange, convection and the storage of latent-heat in animal coats. *Agricultural and Forest Meteorology* **53**, 325–336.

McArthur, A. J. & Monteith, J. L. (1980). Air movement and heat loss from sheep. II. Thermal insulation of fleece in wind. *Proceedings of the Royal Society of London. Series B, Biological Sciences* **209**, 209–217.

McDowell, R. E., McDaniel, B. T. & Hooven, N. W. (1958). Relation of the rhomboideus (hump) muscle in zebu and European type cattle. *Journal of Animal Science* **17**, 1229 (abstract).

McGovern, R. E. & Bruce, J. M. (2000). A model of the thermal balance for cattle in hot conditions. *Journal of Agricultural Engineering Research* **77**, 81–92.

Mitloehner, F. M. & Laube, R. B. (2003). Chronobiological indicators of heat stress in *Bos indicus* cattle in the tropics. *Journal of Animal and Veterinary Advances* **2**, 654–659.

Monteith, J. L. (1973). *Principles of Environmental Physics*, 1st edn, London: Edward Arnold.

Monteith, J. L. & Unsworth, M. H. (2008). *Principles of Environmental Physics*, 3rd edn, Burlington, MA: Academic Press.

Murray, F. W. (1967). On the computation of saturation vapor pressure. *Journal of Applied Meteorology* **6**, 203–204.

Myers, G. E. (1971). *Analytical Methods in Conduction Heat Transfer*. New York: McGraw-Hill.

NRC (1984). *Nutrient Requirements of Beef Cattle*, 6th edn, Washington, DC: National Academy Press.

NRC (2000). *Nutrient Requirements of Beef Cattle*, 7th edn, Washington, DC: National Academy Press.

O'Connor, M. P. & Spotila, J. R. (1992). Consider a spherical lizard: animals, models, and approximations. *American Zoologist* **32**, 179–193.

Olson, R. M. (1962). *Essentials of Engineering Fluid Mechanics*. Scranton, PA, USA: International Textbook Co.

Oyarzun, R. A., Stockle, C. O. & Whiting, M. D. (2007). A simple approach to modeling radiation interception by fruit-tree orchards. *Agricultural and Forest Meteorology* **142**, 12–24.

Pan, Y. S. (1963). Quantitative and morphological variation of sweat glands, skin thickness, and skin shrinkage over various body regions of Sahiwal Zebu and Jersey cattle. *Australian Journal of Agricultural Research* **14**, 424–437.

Peterson, T. C. & Parton, W. J. (1983). Diurnal-variations of wind speeds at a shortgrass prairie site – a model. *Agricultural Meteorology* **28**, 365–374.

Porter, W. P. & Gates, D. M. (1969). Thermodynamic equilibria of animals with environment. *Ecological Monographs* **39**, 227–244.

Sen, Z. (2008). *Solar Energy Fundamentals and Modeling Techniques: Atmosphere, Environment, Climate Change, and Renewable Energy*. London: Springer.

Shampine, L. F., Reichelt, M. W. & Kierzenka, J. A. (1999). Solving index-1 DAEs in MATLAB and Simulink. *SIAM Review* **41**, 538–552.

Singh, G., Gaur, G. K., Nivsarkar, A. E., Patil, G. R. & Mitkari, K. R. (2002). Deoni cattle breed of India. A study on population dynamics and morphometric characteristics. *Animal Genetic Resources Information* **32**, 35–43.

Stolwijk, J. A. J. & Hardy, J. D. (1966). Temperature regulation in man – a theoretical study. *Pflügers Archiv (European Journal of Physiology)* **291**, 129–162.

Takada, S., Kobayashi, H. & Matsushita, T. (2009). Thermal model of human body fitted with individual characteristics of body temperature regulation. *Building and Environment* **44**, 463–470.

Thom, E. C. & Bosen, J. F. (1959). The discomfort index. *Weatherwise* **12**, 57–60.

Thomas, C. K. & Pearson, R. A. (1986). Effects of ambient-temperature and head cooling on energy-expenditure, food-intake and heat tolerance of Brahman and Brahman x

Friesian cattle working on treadmills. *Animal Production* **43**, 83–90.

Thompson, V. A., Fadel, J. G. & Sainz, R. D. (2011). Meta-analysis to predict sweating and respiration rates for *Bos indicus, Bos taurus*, and their crossbreds. *Journal of Animal Science* **89**, 3973–3982.

Thompson, V. A., Sainz, R. D., Strathe, A. B., Rumsey, T. R. & Fadel, J. G. (in press). *The evaluation of a dynamic, mechanistic, thermal balance model for Bos indicus and Bos taurus*. Cambridge: Journal of Agricultural Science.

Turco, S. H. N., da Silva, T. G. F., de Oliveira, G. M., Leitão, M. M. V. B. R., de Moura, M. S. B., Pinheiro, C. & Padilha, C. V., da, S. (2008). Estimating black globe temperature based on meteorological data. In *Livestock Environments VIII. Proceedings of the Eighth ASABE International Livestock Environment Symposium, 31 August – 4 September 2008, Iguassu, Brazil*, pp. 783–788. St. Joseph, MI, USA: ASABE.

Turnpenny, J. R., McArthur, A. J., Clark, J. A. & Wathes, C. M. (2000*a*). Thermal balance of livestock 1. A parsimonious model. *Agricultural and Forest Meteorology* **101**, 15–27.

Turnpenny, J. R., Wathes, C. M., Clark, J. A. & McArthur, A. J. (2000*b*). Thermal balance of livestock 2. Applications of a parsimonious model. *Agricultural and Forest Meteorology* **101**, 29–52.

Vera, R. R., Koong, L. J. & Morris, J. G. (1975). A model of heat flow in the sheep exposed to high levels of solar radiation. *Computer Programs in Biomedicine* **4**, 214–218.

Voelker, C., Hoffmann, S., Kornadt, O., Arens, E., Zhang, H. & Huizenga, C. (2009). Heat and moisture transfer through clothing. In *Building Simulation 2009: Proceedings of the 11th IBPSA Conference, Glasgow, Scotland, 27–30 July 2009*, pp. 1360–1366. Glasgow, UK: IBPSA. Available from: http://www.ibpsa.org/m_bs2009.asp (verified 30 May 2013).

Zhang, J. H., Gupta, A. & Baker, J. (2007). Effect of relative humidity on the prediction of natural convection heat transfer coefficients. *Heat Transfer Engineering* **28**, 335–342.